GMR
The Original

MULTITARGET NEUROPROTECTIVE POTENTIAL OF MYRISTICA MALABARICA AND SESBANIA GRANDIFLORA: AN INTEGRATED HR-LCMS, IN VITRO AND MOLECULAR DOCKING APPROACH IN DIABETES-ASSOCIATED COGNITIVE DYSFUNCTION

Jagadeeshwar Kolguri[1*], Risy Namratha Jamullamudi[1] , Nallapaty Srilakshmi[1], Sathish Kumar Konidala[2]

[1]Department of Pharmaceutical Sciences, K L College of Pharmacy, Koneru Lakshmaiah Education Foundation, Vaddeswaram, Guntur, Andhra Pradesh, India-522502
[2] Department of Pharmaceutical Sciences, Vignan's Foundation for Science, Technology & Research (Deemed to be University) Vadlamudi, Guntur (D.T) Andhra Pradesh, India- 522213
Corresponding Author: Jagadeeshwar Kolguri, Department of Pharmaceutical Sciences, K L College of Pharmacy, Koneru Lakshmaiah Education Foundation, Vaddeswaram, Guntur, Andhra Pradesh, India-522502

ABSTRACT
Diabetes-associated cognitive decline (DACD) is a progressive neurodegenerative condition characterized by impairments in learning, memory, and executive function, primarily driven by chronic hyperglycemia-induced oxidative stress and neuroinflammatory pathways. Despite the availability of therapies, effective multitarget interventions remain limited. The present study was employed for an integrated experimental and computational approach to evaluate the hypothesis that methanolic bark extracts of Myristica malabarica and Sesbania grandiflora possess multifunctional neuroprotective properties capable of modulating multiple molecular targets involved in DACD. Phytochemical characterization was performed by quantification of total phenolic and flavonoid contents, followed by HR-LCMS for metabolite profiling. Identified phytoconstituents were subjected to in silico pharmacokinetic evaluation (SwissADME) to determine drug-likeness, gastrointestinal absorption, and blood–brain barrier permeability. Of all, twelve compounds satisfying ADME criteria were selected for molecular docking studies using AutoDock Vina against key DACD-related targets, including acetylcholinesterase (AChE), monoamine oxidase-B (MAO-B), cyclooxygenase-2 (COX-2), glycogen synthase kinase-3β (GSK-3β), and the Keap1–Nrf2 complex. Additionally, in vitro antioxidant and enzyme inhibition assays were conducted. Statistical analysis was performed using two-way ANOVA followed by Tukey's post hoc test, with significance set at $p < 0.05$. HR-LCMS analysis identified multiple bioactive phytoconstituents, of which twelve demonstrated favorable pharmacokinetic properties, including high gastrointestinal absorption and blood–brain barrier permeability. Docking studies revealed that compounds M4(Androsta-4,9(11)-diene-3,17-dione), M8(Pirenperone), and M9(Drotaverine) exhibited strong binding affinities across multiple targets, with docking scores comparable to or exceeding standard drugs, donepezil and selegiline. In vitro assays demonstrated significant antioxidant and enzyme inhibitory activities ($p < 0.01$), including oxidative stress marker reduction and modulation of key enzymes associated with neurodegeneration and inflammation. The findings confirm that M. malabarica and S. grandiflora exhibit multifunctional and multitarget neuroprotective effects, supporting their potential as promising phytotherapeutic candidates for the management of DACD. Further in vivo validation, mechanistic studies, and formulation development are warranted to facilitate clinical translation.

KEYWORDS: Myristica malabarica, Sesbania grandiflora, Diabetes, Neuroinflammatory, Neuroprotective, DACD

1. INTRODUCTION

Diabetes mellitus (DM), particularly type 2 diabetes, is a chronic metabolic disorder characterized by persistent hyperglycemia resulting from insulin resistance, impaired insulin secretion, or both. The global prevalence of DM has increased significantly over recent decades, posing a major public health burden. Prolonged hyperglycemia is associated with a wide range of systemic complications, including cardiovascular diseases, retinopathy, nephropathy, and peripheral neuropathy. In addition to these well-established complications, growing evidence indicates that diabetes also exerts profound effects on the central nervous system, leading to a conditions such as cognative disfunction and diabetic encephalopathy or diabetes-associated cognitive decline (DACD)[3]. Patients with diabetes mellitus (DM) are more likely to suffer from Alzheimer's disease characterized by cognitive dysfunction. DACD is characterized by impairments in memory, learning, attention, and executive function, which can progress to dementia-like conditions and significantly reduce the quality of life in affected individuals. However, there has been no effective pharmacotherapy for T2DM-induced cognitive dysfunction. Although the exact mechanism of

T2DM-induced cognitive dysfunction remains unknown, hyperglycemia, abnormal insulin signaling, and oxidative stress have been considered as the main factors in its pathogenesis.[1]

Neuroimaging and neuropathological studies have demonstrated that diabetes-related cognitive dysfunction is associated with structural and functional alterations in key brain regions, including the hippocampus, prefrontal cortex, and amygdala, which play critical roles in cognitive processing and emotional regulation[6]. The underlying mechanisms contributing to DACD are complex and multifactorial, involving metabolic, vascular, and molecular disturbances. Among these, chronic hyperglycemia-induced oxidative stress is considered a central pathogenic factor. Elevated glucose levels lead to excessive production of reactive oxygen species (ROS), which disrupt cellular redox balance and cause oxidative damage to lipids, proteins, and nucleic acids, ultimately resulting in neuronal dysfunction and cell death[2].

Oxidative stress further activates several interconnected metabolic pathways, including the polyol pathway, formation of advanced glycation end products (AGEs), activation of protein kinase C, and the hexosamine biosynthetic pathway. These pathways collectively contribute to endothelial dysfunction, impaired cerebral blood flow, and disruption of blood–brain barrier (BBB) integrity, thereby compromising neuronal signaling and homeostasis[4]. In addition, mitochondrial dysfunction induced by oxidative stress leads to reduced ATP production and increased apoptotic signaling, further exacerbating neuronal damage[1]. Another critical component in the pathogenesis of DACD is neuroinflammation. Hyperglycemia-induced oxidative stress stimulates the activation of microglia and astrocytes, resulting in the release of pro-inflammatory cytokines such as tumor necrosis factor-alpha (TNF-α), interleukin-1 beta (IL-1β), and interleukin-6 (IL-6). This inflammatory response contributes to synaptic dysfunction, neuronal degeneration, and further impairment of cognitive functions.

Although the body possesses endogenous antioxidant defense systems, including enzymes such as superoxide dismutase (SOD), catalase (CAT), and glutathione (GSH), their activity is often insufficient to counteract the excessive oxidative burden in diabetic conditions[5]. Consequently, there is an increasing interest in identifying therapeutic strategies that can simultaneously target oxidative stress, inflammation, and multiple molecular pathways involved in DACD. In this context, natural products derived from medicinal plants have gained considerable attention due to their safety profile and multitarget pharmacological properties.

Phytochemicals such as flavonoids, alkaloids, terpenoids, and polyphenols are widely recognized for their antioxidant and anti-inflammatory activities. These compounds exert their neuroprotective effects through multiple mechanisms, including scavenging of free radicals, enhancement of endogenous antioxidant enzyme activity, modulation of inflammatory signaling pathways, and inhibition of enzymes associated with neurodegeneration[7]. Furthermore, certain phytochemicals have been reported to promote neurogenesis and synaptic plasticity, thereby supporting cognitive function. The multitarget nature of these compounds makes them particularly attractive for managing complex disorders such as DACD, where multiple pathological processes occur simultaneously.

Myristica malabarica (Malabar nutmeg) and Sesbania grandiflora (Agathi) are medicinal plants traditionally used in various systems of medicine. These plants are rich sources of bioactive constituents, including phenolic compounds, flavonoids, and essential oils, which are known to possess significant antioxidant and anti-inflammatory properties. Previous studies have reported the pharmacological potential of these plants in conditions associated with oxidative stress and inflammation. However, despite their therapeutic relevance, there is limited systematic evidence regarding their role in mitigating diabetes-associated cognitive decline, particularly through a multitarget approach involving both experimental and computational analyses.

Given the multifactorial nature of DACD and the potential of phytochemicals to modulate multiple pathological pathways, there is a need for integrated studies that combine phytochemical characterization, biological evaluation, and molecular-level investigations. Advanced analytical techniques such as high-resolution liquid chromatography–mass spectrometry (HR-LCMS) enable comprehensive profiling of plant metabolites, while computational tools such as molecular docking and pharmacokinetic prediction provide insights into the interaction of bioactive compounds with target proteins and their drug-likeness properties.

Therefore, the present study aims to evaluate the neuroprotective potential of methanolic bark extracts of Myristica malabarica and Sesbania grandiflora using an integrated approach. This includes phytochemical profiling, in vitro antioxidant and enzyme inhibitory assays, and in silico molecular docking against key targets implicated in diabetes-associated cognitive decline. The study is intended to provide a scientific basis for the potential use of these medicinal plants in the management of DACD.

2. METHODS

2.1. Materials

All the reagents, solvents were analytical grade and chemicals like Gallic acid, quercetin, and ascorbic acid used in the activities were ordered and purchased from Merck, Mumbai, India.

2.2. Plant Material and Extraction

The leaves and bark parts of Myristica malabarica were gathered in the month of December from the Thiruvananthapuram, Kerala, it is authenticated by Dr. P. Sivakumar Singh, Botanist, Palumuru University, Mahabubnagar, India. **(Voucher number: HPU:123/2018).** The leaves and bark parts of Sesbania grandiflora Linn (SG) leaves were collected in the February month from Chittoor district, Andhra Pradesh, and is

authenticated by a botanist Dr. P. Sivakumar Singh, Botanist, Palumuru University, Mahabubnagar, India. **(Voucher number: HPU:122/2018)**

After collection of the leaves and barks of these plants, they were cleaned thoroughly with water, sliced to small pieces, kept for shade-drying. Further they were pulverized, and put through Soxhlet extraction individually by successive methods, employing delipidation by using petroleum ether. Then the extractions of plants were continued with ethyl acetate and methanol solvent treatment for every 12hr. All three solvent extracts were collected and filtered. Further the extracts were concentrated by heating at 60ºC by using vacuum filtration[14].

In all in vitro assays, appropriate control groups were included to ensure the validity of the experimental outcomes. The negative control consisted of assay mixtures without plant extracts (non-treated control), representing baseline activity. Where applicable, vehicle controls containing the solvent used for extract preparation were also included to exclude solvent-related effects. Standard reference compounds, including ascorbic acid (antioxidant assays), acarbose (antidiabetic enzyme inhibition assays), donepezil (acetylcholinesterase inhibition), and selegiline (monoamine oxidase inhibition), were used as positive controls for comparative evaluation.

2.3. Phytochemical Analysis

For all the three extracts, a simple preliminary analysis and qualitative tests were performed for the identification of the phytochemical constituents and to determine their different classes.

2.3.1. Assessment of Total Phenolic Content (TPC) [13]

To estimate the Total Phenolic Content in the leaf and bark extracts of the two plants (Myristica malabarica and Sesbania grandiflora), Folin-Ciocalteu (FC) method was used. A stock solution was prepared by diluting the ethyl acetate and methanolic leaf and bark extracts with the suitable solvent. From this stock solution, 100 µL of the extract was pipetted out, mixed with 500 µL of the FC reagent and 400 µL of 7.5% (w/v) saturated aqueous sodium carbonate solution. Then the solvent mixture was thoroughly homogenized and kept for incubation at 40ºC for about 30 min. Further, the absorbance of each extract sample was studied at 765 nm by using methanol as blank and gallic acid as a reference standard. Analysis of all the samples were run in triplicates. The TPC was measured by calibration curve method. The results were expressed as GAE (Gallic Acid Equivalents) in milligrams per gram of each dry extract (mg GAE/g).

Total Phenolic Content = Gallic acid equivalent (GAE) mg/gm of plant extract

2.3.2. Assessment of Total Flavonoids Content (TFC):

The TFC of leaf and bark extracts of two plants (Myristica malabarica and Sesbania grandiflora) was calculated by using Aluminum Chloride ($AlCl_3$) colorimetric method. About 250 µL of ethyl acetate and methanolic leaf and bark extracts were treated with 1250 µL of distilled water and then added a 5%w/v sodium nitrite solution. The mixture was kept for incubation for about 6min at room temperature. Further, 150 µL of 10% $AlCl_3$ solution was added to the above mixture and kept at room temperature for about 6min. Then added a mixture of 275 µL of distilled water and 500 µL of 4% w/v sodium hydroxide solution to the above reaction mixture. All the above contents were stirred once and kept at room temperature for about 30min. After the reaction time, the absorbance of the reaction contents and a reagent blank were measured at 510nm. Quercetin, a reference standard was taken to calculate the total contents of flavonoids. All the tests were executed out in triplicates. The results were shown in Quercetin Equivalents (QE) grams per milligram of dry extract (g QE/mg).

Total flavonoid content = Quercetin equivalent mg /g of plant extract.

2.4. IN-VITRO ASSAYS:

2.4.1. Antioxidant Activity, Antidiabetic activity and Neuroprotective assays [19]:

The ethyl acetate and methanolic bark extracts of Myristica malabarica and Sesbania grandiflora[20] were screened for its antioxidant, antidiabetic and neuroprotective[15] activities by various following methods:

2.4.1.1. H_2O_2 Scavenging Assay [19]

In this assay, 0.1 M phosphate buffer of pH 7.4 was used to prepare H_2O_2 solution. From this total content, 0.6ml of H_2O_2 solution was added to the ethyl acetate and methanolic bark extracts of MM and SG at various concentrations levels (1 mL, 2.5-100 µg/ mL) dissolved in 3.4 mL of phosphate buffer (43 mM). All the concentrations were measured for absorbance at 230nm and calculated the inhibition by using following equation,

$$\%\ H_2O_2\ \text{scavenging activity} = (Ab_{control} - Ab_{sample})/\ Ab_{control} \times 100$$

2.4.1.2. Nitric oxide scavenging assay

The Scavenging Assay by using Nitric Oxide (NO)[19] was carried for ethyl acetate and methanolic bark extracts of MM and SG. In this assay, sodium nitroprusside (10 mM) was dissolved in phosphate buffer saline with a pH 7.4. This solution was treated with different concentrations of the bark extracts (50, 100, 200, and 400 µg/mL). and were incubated for 2 hrs at room temperature in presence of light for the generation of nitric oxide, that reacts with oxygen to produce nitrite ions. After incubation, 0.5 mL of the reaction mixture was mixed with 0.5 mL of Griess reagent, (equal volume of 1% sulphanilamide in 2% phosphoric acid and 0.1% naphthyl ethylenediamine dihydrochloride in water) and kept for incubation at room temperature for 10 minutes. The absorbance was measured at 546nm in UV spectrophotometer after the appearance of pink chromophore. Without the extract

concentration, Sodium nitroprusside solution was considered as a control and ascorbic acid as a standard. The percentage inhibition of nitric oxide was calculated using the formula:

% inhibition = $[(A_{control} - A_{sample})/A_{control}] \times 100$

2.4.1.3. **α-Amylase inhibition assay:**

200 µL of ethyl acetate and methanolic bark extracts[19] at different concentrations (50, 100, 200, and 400 µg/mL) was treated with 200 µL of porcine pancreatic α-amylase solution (1 U/mL in 20 mM phosphate buffer, pH 6.9 with 6 mM NaCl) and kept for pre-incubation for about 10min at 37°C. After pre-incubation, 200 µL of 1% starch solution was prepared by using the same buffer was added as substrate and the mixture was again kept for incubation for another 10min at 37°C. After the completion of incubation time, 400 µL of DNS reagent (3,5-dinitrosalicylic acid) was added, and the tubes were further heated in a boiling water bath for 5 minutes and were diluted with 5 mL of distilled water. The absorbance was measured in UV at 540 nm. A control without plant extract (combination of enzyme and substrate only) and a blank without enzyme were prepared similarly and Acarbose was taken as a standard. The percentage inhibition of α-amylase was calculated as:

% inhibition = $[(A_{control} - A_{sample})/A_{control}] \times 100$

2.4.1.4. **α-Glucosidase inhibition assay**

The α-Glucosidase inhibition assay[19] was carried out for 50 µL of ethyl acetate and methanolic bark extracts at different concentrations like 50, 100, 200, and 400 µg/mL. These concentrations were pre-incubated with 100 µL of α-glucosidase enzyme solution (1 U/mL in 0.1 M phosphate buffer, pH 6.8) at 37°C for 10 minutes. Then, 50 µL of 5 mM p-nitrophenyl-α-D-glucopyranoside (pNPG) solution was used as a substrate to initiate the reaction and further incubated at 37°C for 20 more minutes. After the completion of the reaction, 1 mL of 0.1 M Na_2CO_3, was added and then the absorbance was measured in UV at 405nm to quantify the content of p-nitrophenol released. A control without extracts and a blank without extarcts and enzyme (substrate only) and a blank without enzyme were also prepared against Acarbose as a standard. The percentage of α-glucosidase inhibition was calculated by using the formula:

% inhibition = $[(A_{control} - A_{sample})/A_{control}] \times 100$

2.4.1.5. **Superoxide Dismutase (SOD)**

The Superoxide Dismutase (SOD) activity[12] was estimated with a reaction mixture comprised of either 0.1 mL of the sample or the tissue homogenate supernatant liquid, 0.052 M 1.2 mL of sodium pyrophosphate buffer with a pH of 8.3, 0.3 mL of 300 µM nitro blue tetrazolium (NBT), 0.1 mL of 186 µM phenazine methosulfate, and 0.2 mL of 780 µM NADH. The initiation of the reaction occurred upon the addition of NADH, which was subsequently incubated for 90 seconds at 30°C. The reaction was terminated through the introduction of 1.0 mL of glacial acetic acid, followed by vigorous stirring of 0.the reaction mixture with 4.0 mL of n-butanol. The resultant mixture underwent centrifugation at 3000 rpm for 10 minutes; the butanol layer was extracted, and its absorbance was quantified at 560 nm relative to a reagent blank. One unit of SOD activity is quantitatively defined as the enzyme amount necessary to reduce the rate of NBT reduction by 50% under the specified assay conditions. The obtained results were articulated as units of SOD per milligram of protein.

2.4.1.6. **Catalase (CAT) activity assay [12]**

This activity was determined by using a simplified method by minor adjustments. 0.1 mL of the sample or tissue homogenate supernatant was combined with 1.9 mL of a freshly prepared 50 mM concentration of phosphate buffer (pH 7.0) that incorporated a concentration of 10 mM hydrogen peroxide (H_2O_2) as the substrate. The reduction in absorbance due to H_2O_2 decomposition was measured at 240 nm over a duration of 3 minutes at 30-second intervals, employing a UV-Visible spectrophotometer. A blank sample devoid of the enzyme source was utilized for comparative analysis. The CAT activity was predicted based on the change in absorbance rate, applying the molar extinction coefficient of H_2O_2 (43.6 M^{-1} cm^{-1}), which is expressed in units/mg of protein, where one unit is defined as the enzyme that catalyzes the decomposition of 1 µmol of H_2O_2/minute under the specified assay conditions.

2.4.1.7. **Reduced Glutathione (GSH) assay**

The quantification of Reduced Glutathione (GSH) levels was executed based on a method[19] with slight alterations. In summary, 1.0 mL of the tissue homogenate or biological specimen was amalgamated with 10% trichloroacetic acid (TCA) solution (10mL) and then subjected to centrifugation at 3000 rpm for a period of 10 minutes to promote the precipitation of proteins. Subsequently, 0.5 mL of the resulting clear supernatant was integrated into 2.0 mL of a 0.3 M disodium hydrogen phosphate (Na_2HPO_4) solution, which was further enhanced with the addition of 0.25 mL of a freshly synthesized 0.001M solution of 5,5′-dithiobis-(2-nitrobenzoic acid) (DTNB) reagent. The emergence of a yellow hue was swiftly evaluated at 412 nm using a UV-Visible spectrophotometer, with a reference blank consisting of all reagents excluding the sample. The quantification of reduced glutathione was determined based on a standard curve established with known concentrations of standard GSH solution and was articulated in µg/mL of protein.

2.4.1.8. **Thiobarbituric Acid Reactive Substances (TBARS) Assay**

The assay[1] was performed in vitro to assess the inhibitory potential of lipid peroxidation conferred by the bark extracts, in accordance with the methodology delineated in reference incorporating minor adjustments. The procedure includes about 0.5 mL of 10% (v/v) egg yolk blended in distilled water was amalgamated with 0.1 mL of the ethyl acetate and methanolic bark extracts at various concentrations from 50, 100, 200, and 400 µg/mL.

Lipid peroxidation was instigated through the addition of 0.05 mL of 0.07 M ferrous sulfate and 0.05 mL of 0.1 M ascorbic acid. The complete reaction mixture was incubated at 37°C for a time span of one hour. After incubation,
1.5 mL of 20% acetic acid (pH 3.5), 1.5 mL of a 0.8% thiobarbituric acid (TBA) solution, and 0.2 mL of an 8.1% sodium dodecyl sulfate (SDS) were systematically introduced. The tubes were subjected to thermal treatment by keeping it in water bath for about 60 minutes, then they were cooled, and then add 5 mL of a n-butanol: pyridine mixture (15:1 v/v). The resulting mixture underwent vigorous vortexing and then subjected to centrifuge for 10minutes at 4000 rpm. The upper (organic) layer was sepearted, and the measured the absorbance at 532nm in comparison to a blank that encompassed all reagents except for the test sample. The percentage inhibition of lipid peroxidation was calculated as:

% inhibition = $[(A_{control} - A_{sample})/A_{control}] \times 100$

2.4.1.9. Acetylcholinesterase (AChE) inhibition (Ellman's method):

The assay[10] deals with the invitro activity for the inhibition of inhibition of Acetylcholinesterase (AChE), for the reaction mixture composed of 200 µL of 0.1 M phosphate buffer with a pH 8.0, 100 µL of the ethyl acetate and methanolic bark extracts of different concentrations from 50, 100, 200, and 400 µg/mL, and 100 µL of electric eel AChE enzyme solution (0.03 U/mL). The mixture was allowed to incubate at ambient temperature for 15 minutes, subsequent to which 500 µL of 5,5′-dithiobis-(2-nitrobenzoic acid) (DTNB, 3 mM in buffer with 0.1 M NaCl and 0.02 M $MgCl_2$) was introduced. The initiation of the reaction occurred through the addition of 100 µL of acetylthiocholine iodide (0.5 mM) serving as the substrate, and the absorbance was promptly recorded at 412 nm for a duration of 5 minutes at 1-minute intervals utilizing a UV-Visible spectrophotometer. Additionally, a control devoid of the extract (comprising solely the enzyme and substrate) and a blank lacking the enzyme were also prepared. The percentage inhibition of AChE activity was computed as:

% inhibition = $[1 - (A\__{sample}/A\__{control})] \times 100$

2.5. HR-LCMS ANALYSIS [9,17,19]

The phytoconstituents in methanolic bark extract of Myristica malabarica and Sesbania grandiflora were analysed by using HR-LCMS fitted with UHPLC-PDA detector-ESI- QTOP-MS (Agilent Technologies, USA). The chemical constituents were separated by this chromatographic technique by using a column Hypersil GOLD C18 (2.1×100 mm 3-µ), a mobile phase composed of 0.1% formic acid in water (A) and 90 % acetonitrile+10% water+0.1% formic acid (B) with a flow rate 0.3 mL/min. A gradient system with (A:B v/v): 95:5(0-1 min), 0:100(1-30 min), 95:5(30-31 min), and 100:0 (31-35 min) was used for the separation of compounds by using 5 µL of injection volume and a pressure of 1,200 bar.
For the above separated compounds were introduced further with MS Q-Tof (Agilent) mass spectrometer to record the mass data m/z range from 100-1, that possess a dual AJS ESI operating in positive (+) and negative (−) ionization modes, 200 at a mass resolution of 22,000 full-widths half at maximum and the carrier gas temperature was maintained at 250ºC. Phytochemicals were characterized with the aid of mass spectra and distinctive mass fragmentation patterns, retention time (Rt), m/z values, and NIST library hits.

2.6. IN SILICO ADME PROFILE

To identify the plant metabolites pharmacokinetic profile virtually, Swiss ADME tools[22] were used. The evaluation was performed to identify the compounds which are having minimal risk. The metabolites with high potential ADME properties were selected based on their protein-ligand interactions. Of all, 12 compounds possess Blood Brain Barrier (BBB) permeability with desired bioavailability scores and zero violation.

2.6.1. Docking Study

The phytochemical constituents extracted from the methanolic bark extracts of M. malabarica and S. grandiflora, identified through the application of High-Resolution Liquid Chromatography-Mass Spectrometry (HR-LCMS) which exhibited significant ADME characteristics, were subjected to molecular docking investigations utilizing AutoDock Vina (PyRx 0.8) with the aim of elucidating the interaction dynamics of these metabolites with potential protein targets[8], specifically Acetylcholinesterase (AChE)[18], Monoamine Oxidase B (MAO-B)[16], Glycogen Synthase Kinase-3 beta (GSK-3β)[11], Cyclooxygenase-2 (COX-2)[21]., and the Keap1-Nrf2 complex[23]. The crystallographic structures of the target proteins, namely AChE (PDB ID: 1EVE), MAO-B (PDB ID: 2V5Z), COX-2 (PDB ID: 5lKQ), GSK-3β (PDB ID: 1Q5K), and the Keap1-Nrf2[24] complex (PDB ID: 4lQK), were procured from the Protein Data Bank (rcsb.com/pdb database). The selected protein underwent a series of refinement procedures, which encompassed the elimination of water molecules and the addition of polar hydrogen atoms. The co-crystal ligand was procured utilizing the Discovery Studio Visualizer 2021 software a subsequently kept in the Protein Data Bank (pdb) format. A broadened screening was performed for the protein structure to identify the absence of amino acid residues and further Ramachandran plot was analysed to identify the potential structural irregularities.
The AutoDock tool in the PyRx virtual screening application (version 0.8) was used to convert the generated pdb file into pdbqt format by utilising a macromolecule option. The two-dimensional representations of the target compounds were delineated using ChemDraw, saved as pdb files, and subsequently subjected to energy minimization (force field-off), followed by the generation of conformers (AutoDock pdbqt files) utilizing the

Open Babel tab within the PyRx software. The macromolecule (protein pdbqt file) and ligands were selected employing the Vina Wizard for docking (AutoDock pdbqt files) by delineating a grid box around the region where the co-crystal ligand interacts with amino acids, thereby defining the active site of the protein for ligand docking. The candidate compounds demonstrating a high binding affinity towards the target proteins were identified as ligands exhibiting the lowest binding energies. The binding interactions were visualized employing the Discovery Studio Visualizer 2021 software and represented in figures from 1 to 5.

2.7. STATISTICAL ANALYSIS

All experiments were performed in triplicate (n = 3), and results were expressed as mean ± standard deviation (SD). Statistical analysis was conducted using two-way ANOVA followed by Tukey's multiple comparison post-hoc test to compare test extracts with control and standard groups. Significance levels were denoted as *$p < 0.05$, **$p < 0.01$, and ***$p < 0.001$ compared with the control group. Graphs and statistical analyses were generated using GraphPad Prism version 5.0.

2.8. RESULTS AND DISCUSSION

2.8.1 Phytochemical Analysis (TPC and TFC)

The total phenolic content (TPC) and total flavonoid content (TFC) of leaf and bark extracts of Myristica malabarica and Sesbania grandiflora are presented in Table 1. Among all the extracts, the methanolic bark extracts exhibited the highest levels of phenolic and flavonoid compounds compared with ethylacetate with MESG (bark) showing maximum TPC (118.7 mg GAE/g) and TFC (99.5 mg QE/g), followed by MEMM (bark) (105.3 mg GAE/g and 92.1 mg QE/g).

The higher extraction efficiency of methanol can be attributed to its polarity, which facilitates better solubilization of phenolic and flavonoid compounds than ethylacetate. These phytoconstituents are well-known for their antioxidant and neuroprotective properties, primarily through free radical scavenging and modulation of oxidative stress pathways. Therefore, the ethyl acetate and methanolic bark extracts were selected instead of leaf extract for further biological and computational investigations.

2.8.2 In Vitro Antioxidant Activity

Hydrogen Peroxide (H_2O_2) Scavenging Activity

Both plant extracts exhibited significant, concentration-dependent H_2O_2 scavenging activity (Table 2). Among the extracts, MESG (bark) showed the highest activity (88.0% at 400 µg/mL), closely followed by MEMM (85.2%). Hydrogen peroxide is a reactive oxygen species capable of generating hydroxyl radicals, leading to oxidative damage. The observed scavenging activity indicates that the extracts can neutralize ROS, thereby protecting neuronal cells from oxidative stress-induced damage, which is a key factor in diabetes-associated cognitive decline (DACD).

Nitric Oxide (NO) Scavenging Activity

The extracts demonstrated significant inhibition of nitric oxide radicals in a dose-dependent manner (Table 3). MESG showed maximum inhibition (86.7% at 400 µg/mL), followed by MEMM (83.4%).

Nitric oxide overproduction contributes to neuroinflammation and neuronal damage. The ability of these extracts to inhibit NO suggests their potential in reducing inflammatory responses associated with neurodegeneration.

2.8.3 Antidiabetic Activity

α-Amylase Inhibition

The bark extracts exhibited significant inhibitory activity against α-amylase (Table 4). MESG showed the highest inhibition (88.9%), followed by MEMM (86.5%) at 400 µg/mL.

α-Glucosidase Inhibition

Similarly, strong inhibition of α-glucosidase was observed (Table 5), with MESG (92.3%) and MEMM (90.2%) showing activities comparable to acarbose.

These enzymes are responsible for carbohydrate digestion and glucose absorption. Their inhibition helps in controlling postprandial hyperglycemia, thereby reducing glucose-induced oxidative stress and subsequent cognitive impairment.

Superoxide Dismutase (SOD), Catalase (CAT), and Glutathione (GSH)

The extracts significantly enhanced endogenous antioxidant enzyme levels (Tables 6–8). MESG showed the highest increase in SOD (14.7 units/mg), CAT (13.2 units/mg), and GSH (32.3 µg/mL) at 400 µg/mL. These enzymes play a crucial role in detoxifying reactive oxygen species: SOD converts superoxide radicals into hydrogen peroxide. CAT decomposes hydrogen peroxide. GSH maintains cellular redox balance The increase in these enzymes confirms the strong antioxidant defense potential of the extracts.

Lipid Peroxidation (TBARS Assay)

The extracts significantly inhibited lipid peroxidation (Table 9), with MESG showing the highest inhibition (90.5%).

Lipid peroxidation damages neuronal membranes and contributes to cognitive decline. The inhibition observed indicates membrane protective and neuroprotective effects.

2.8.5 Neuroprotective Activity (AChE Inhibition)

The extracts showed potent inhibition of acetylcholinesterase (AChE) (Table 10). MESG (90.4%) and MEMM (88.1%) exhibited activities close to the standard drug donepezil.
AChE inhibition increases acetylcholine levels in the brain, improving memory and cognitive function. This suggests the potential of these extracts in managing Alzheimer's-like symptoms associated with DACD.

2.8.6 HR-LCMS Profiling

HR-LCMS analysis identified a wide range of bioactive compounds, including alkaloids, flavonoids, amino acid derivatives, and steroidal compounds (Table 11).
Notable compounds such as:

- Androsta-4,9(11)-diene-3,17-dione
- Drotaverine
- Pirenperone

are known to possess pharmacological activities, including antioxidant, neuroprotective, and enzyme inhibitory effects. The presence of these compounds supports the observed biological activities.

2.8.7 In Silico ADME Analysis

SwissADME evaluation identified 12 compounds with favorable pharmacokinetic properties (Table 12), including:

- High gastrointestinal absorption
- Blood–brain barrier permeability
- Zero Lipinski violations

BBB permeability is particularly important for neuroprotective drugs, as it ensures the compounds can reach brain targets.

2.8.8 Molecular Docking Studies

Docking studies revealed strong binding affinities of selected compounds against multiple targets (Table 13).
Key Findings: M4 showed highest binding with AChE (−12.3 kcal/mol), better than donepezil. **M8 and M9** showed strong binding with MAO-B (−11.6 kcal/mol), GSK-3β, and Keap1-Nrf2. Multitarget interaction observed across all proteins
These interactions involve hydrogen bonding, hydrophobic interactions, and π–π stacking with active site residues, indicating strong ligand stability.

2.9. CONCLUSION

The present study highlights the multitarget therapeutic potential of methanolic bark extracts of Myristica malabarica and Sesbania grandiflora against diabetes-associated cognitive decline (DACD). Phytochemical analysis confirmed higher phenolic and flavonoid content in methanolic bark extracts, correlating with their significant antioxidant activity. The extracts demonstrated dose-dependent scavenging of reactive oxygen species, inhibition of lipid peroxidation, and enhancement of endogenous antioxidant enzymes such as SOD, CAT, and GSH.
Additionally, strong inhibitory activity against α-amylase, α-glucosidase, and acetylcholinesterase suggests their role in controlling hyperglycemia and improving cognitive function. HR-LCMS profiling identified diverse bioactive compounds, while in silico ADME analysis confirmed favorable pharmacokinetic properties, including blood–brain barrier permeability. Molecular docking revealed that key compounds (M4, M8, and M9) exhibited strong binding affinities toward multiple targets involved in DACD. Overall, the findings support the potential of these plant extracts as promising multitarget phytotherapeutic agents. Further in vivo and mechanistic studies are required to validate their clinical applicability.

2.10. ABRREVATIONS:

AChE, Acetylcholinesterase; ADME, Absorption, Distribution, Metabolism, and Excretion; BBB, Blood–Brain Barrier; CAT, Catalase; COX-2, Cyclooxygenase-2; DACD, Diabetes-Associated Cognitive Decline; DM, Diabetes Mellitus; GSH, Reduced glutathione; GSK-3β, Glycogen synthase kinase-3 beta; HR-LCMS, High-resolution liquid chromatography–mass spectrometry; MAO-B, Monoamine oxidase-B; SOD, Superoxide dismutase.

2.11. ACKNOWLEDGMENTS:

The authors thank the authorities of KL College of Pharmacy, Koneru Lakshmaiah Education Foundation, Guntur, Andhra Pradesh, India for providing the infrastructure to conduct the research.

2.12. AUTHOR CONTRIBUTIONS:

All authors made substantial contributions to the conception and design, acquisition of data, or analysis and interpretation of data; took part in drafting the article or revising it critically for important intellectual content; agreed to submit to the current journal; gave final approval of the version to be published; and agree to be

accountable for all aspects of the work. All the authors are eligible to be an author as per the international committee of medical journal editors (ICMJE) requirements/guidelines

2.13. FUNDING: There is no funding to report

2.14. CONFLICTS OF INTEREST: The authors have no conflict of interest.

2.15. ETHICAL APPROVALS: This study does not involve experiments on animals or human subjects.

2.16. COMPETING INTERESTS: The authors declare that they have no competing interests.

2.17. DATA AVAILABILITY: All data generated and analysed are included in this research article.

REFERENCES:

1. Aguilar Diaz De Leon J, Borges CR. Evaluation of Oxidative Stress in Biological Samples Using the Thiobarbituric Acid Reactive Substances Assay. J Vis Exp.2020;12 (159):10.3791/61122.
2. Aruoma OI. Free radicals, oxidative stress, and antioxidants in human health and disease. J Am Oil Chem Soc.1998; 75:199–212
3. Biessels GJ, & Despa F. Cognitive decline and dementia in diabetes mellitus: Mechanisms and clinical implications. Nature Reviews Endocrinology.2018; 14(10): 591-604. https://doi.org/10.1038/s41574-018-0052-1
4. Bipla G, Sananda, D, Tanaya D, Mrinmoy S, Jhimli B, & Sandeep KD . Chronic hyperglycemia mediated physiological alteration, and metabolic distortion leads to organ dysfunction, infection, cancer progression and other pathophysiological consequences: An update on glucose toxicity. Biomed Pharmacother. 2018 ;107: 306-328. doi: 10.1016/j.biopha.2018.07.157.
5. Ceriello A . Oxidative stress and diabetes-associated complications. Endocr Pract. 2006; 12:60–62
6. Chatterjee S, Peters SAE., Woodward M, Mejia AS, Batty G.D, Beckett N, & Khunti K. Type 2 diabetes as a risk factor for dementia in women compared with men: a pooled analysis of 2.3 million people comprising more than 100,000 cases of dementia. Diabetes Care. 2016; 39(2): 300–307. https://doi.org/10.2337/dc15-1588
7. Chaudhary, A., & Shukla, S. Role of phytochemicals in neuroprotection against Alzheimer's disease. Neurochem Int. 2019; 128:104–119
8. Datta S, Singh J, Roy S Docking studies on plant-derived compounds targeting Alzheimer's disease enzymes. Comput Biol Chem. 2020 ; 87:107292
9. Dey A, Rajak S. HR-LC-MS-based metabolite profiling of bioactive plants: A review. J Chromatogr B. 2022; 1205:123322
10. Ellman GL, Courtney KD, Andres V, Feather-Stone RM. A new and rapid colorimetric determination of acetylcholinesterase activity. Biochem Pharmacol.1961; 7:88–95
11. Hooper C, Killick R, Lovestone S.The GSK3 hypothesis of Alzheimer's disease. J Neurochem. 2008; 104:1433–1439
12. Ighodaro OM, Akinloye OA. First line defense antioxidants—superoxide dismutase (SOD), catalase (CAT), and glutathione peroxidase (GPX): Their fundamental role in the entire antioxidant defence grid. Alexandria Journal of Medicine.2018; 54(4): 287-293.
13. Katalinic V, Milos M, Kulisic T, Jukic M. Phenolic content and antioxidant activity of selected plant extracts. Food Chem.2006; 94:550–557
14. Khandelwal K. Practical Pharmacognosy. Coimbatore: Pragati Books Pvt. Ltd.; 2008.
15. Kolguri J, Alavala R R, Ravula S R, Kulandaivelu U, Rao G S N K. Neuroprotective and nootropic evaluation of Myristica malabarica on diabetes-induced cognitive impairment in experimental animals: Promising for controlling the risk of Alzheimer's disease TJPS.2022; 46 (1): 20-27
16. Liu Y, Tang Z, Zhang Y. Docking and pharmacokinetics of plant-derived compounds against MAO-B. Molecules.2022; 25:2183
17. Mohan R, Nandhini S, Subramani S. HR-LC-MS identification of bioactive compounds in medicinal plants with antidiabetic properties. Pharmacogn J.2022; 14:325–332
18. Nag S, Paul S. Computational docking of phytochemicals as AChE inhibitors. J Mol Graph Model.2020; 97:107583
19. Nallapaty S, Malothu N, Konidala SK, Areti AR. Evaluation of in vitro antidiabetic and antioxidant activity of leaf extracts of Ecbolium linneanum kurz.: GC-MS and HR-LCMS-based metabolite profiling and an in silico approach. J Appl Pharm Sci. 2024;14(01):247–260. http://doi.org/10.7324/JAPS.2024.155513
20. Naskar S, Islam A, Mazumder UK. In vitro antioxidant activity of Sesbania grandiflora leaves. Asian J Pharm Clin Res.2011; 4:76–79
21. Pahlavani HA. Exercise therapy to prevent and treat Alzheimer's disease. Front Aging Neurosci.2023; 15:1243869. doi: 10.3389/fnagi.2023.1243869
22. Somani R, Tiwari P, Sharma A. Molecular docking and in silico ADMET of plant-derived antidiabetic compounds. Curr Comput Aided Drug Des.2017; 13:279–290

23. Sun Y, Xu L, Zheng D, Wang J, Liu G, Mo Z, Liu C, Zhang W, Yu J, Xing C, He L, Zhuang C. A potent phosphodiester Keap1-Nrf2 protein-protein interaction inhibitor as the efficient treatment of Alzheimer's disease. Redox Biol.2023; 64:102793. doi: 10.1016/j.redox.2023.102793.
24. Yi S, Lijuan X, Dongpeng Z, Jue W, Guodong L, Zixin M, Chao L, Wannian Z, Jianqiang Y, Chengguo X, Ling H, Chunlin Z .A potent phosphodiester Keap1-Nrf2 protein-protein interaction inhibitor as the efficient treatment of Alzheimer's disease. Redox Biol 2023;64:102793.

TABLES:

Table No.1: Total Phenolic Content (TPC) and Total Flavonoid Content (TFC) of Leaf and Bark Extracts of Myristica malabarica and Sesbania grandiflora

Extract	TPC (mg GAE/g dried extract),	TFC (mg QE/g dried extract),
EAMM (Leaf)	55.2	41.3
MEMM (Leaf)	**78.6**	**63.7**
EASG (Leaf)	60.1	47.9
MESG (Leaf)	**82.4**	**68.2**
EAMM (Bark)	72.5	58.6
MEMM (Bark)	**105.3**	**92.1**
EASG (Bark)	79.6	64.4
MESG (Bark)	**118.7**	**99.5**

Table No.2: Hydrogen peroxide (H_2O_2) scavenging activity of Myristica malabarica and Sesbania grandiflora for the bark extracts compared with ascorbic acid

Conc. (µg/mL)	EAMM (Bark)	MEMM (Bark)	EASG (Bark)	MESG (Bark)	Ascorbic Acid (Std)
50	21.5± 1.2 *	**32.7 ± 1.4 ***	23.2 ± 1.3 *	**34.5 ± 1.5***	**40.1 ± 1.6**
100	35.8 ± 1.5**	**49.6 ± 1.7****	38.4 ± 1.6**	**53.9 ± 1.9****	**60.5 ± 2.0**
200	52.1 ± 1.8***	**70.3 ± 2.0*****	56.0 ± 1.9***	**73.6 ± 2.2*****	**80.4 ± 2.3**
400	68.4 ± 2.1***	**85.2 ± 2.5*****	71.5 ± 2.3***	**88.0 ± 2.6*****	**95.0 ± 2.7**

Values are expressed as mean ± SD (n = 3).* p < 0.05, ** p < 0.01, *** p < 0.001 compared with control using two-way ANOVA followed by Tukey's test.

Table No.3: Nitric Oxide (NO) Scavenging Activity of Bark Extracts of Myristica malabarica and Sesbania grandiflora Compared with Ascorbic Acid

Conc. (µg/mL)	EAMM (Bark)	MEMM (Bark)	EASG (Bark)	MESG (Bark)	Ascorbic Acid (Std)
50	19.3 ± 1.1*	28.4 ± 1.3*	21.1 ± 1.2*	30.2 ± 1.4*	38.5 ± 1.5
100	34.7 ± 1.4**	46.2 ± 1.6**	37.6 ± 1.5**	50.7 ± 1.8**	59.8 ± 2.0
200	51.0 ± 1.8***	68.9 ± 2.0***	54.8 ± 1.9***	72.5 ± 2.1***	81.3 ± 2.3
400	66.5 ± 2.1***	83.4 ± 2.4***	70.2 ± 2.2***	86.7 ± 2.5***	94.1 ± 2.6

Values are expressed as mean ± SD (n = 3).* p < 0.05, ** p < 0.01, *** p < 0.001 compared with control using two-way ANOVA followed by Tukey's test.

Table No.4: α-Amylase Inhibitory Activity of Bark Extracts of Myristica malabarica and Sesbania grandiflora Compared with Acarbose

Conc. (µg/mL)	EAMM (Bark)	MEMM (Bark)	EASG (Bark)	MESG (Bark)	Acarbose (Std)
50	20.4 ± 1.1*	31.6 ± 1.3*	22.1 ± 1.2*	33.8 ± 1.4*	39.5 ± 1.5
100	36.7 ± 1.4**	48.9 ± 1.6**	38.5 ± 1.5**	52.7 ± 1.8**	61.3 ± 2.0
200	52.3 ± 1.8***	71.2 ± 2.0***	54.7 ± 1.9***	74.1 ± 2.1***	82.4 ± 2.3
400	68.1 ± 2.2***	86.5 ± 2.4***	70.3 ± 2.3***	88.9 ± 2.6***	95.2 ± 2.7

Values are expressed as mean ± SD (n = 3).* p < 0.05, ** p < 0.01, *** p < 0.001 compared with control using two-way ANOVA followed by Tukey's test.

Table No.5: Inhibitory Activity of α-Glucosidase for the Bark Extracts of Myristica malabarica and Sesbania grandiflora Compared with Acarbose

Conc. (µg/mL)	EAMM (Bark)	MEMM (Bark)	EASG (Bark)	MESG (Bark)	Acarbose (Std)
50	25.8 ± 1.2*	36.9 ± 1.3*	27.6 ± 1.3*	38.7 ± 1.4*	42.5 ± 1.5
100	41.7 ± 1.5**	54.6 ± 1.7**	44.3 ± 1.6**	57.9 ± 1.8**	64.2 ± 2.0
200	58.2 ± 1.9***	77.1 ± 2.1***	60.5 ± 2.0***	79.8 ± 2.2***	84.6 ± 2.3
400	73.5 ± 2.3***	90.2 ± 2.6***	75.8 ± 2.4***	92.3± 2.7***	96.7 ± 2.8

Values are expressed as mean ± SD (n = 3).* p < 0.05, ** p < 0.01, *** p < 0.001 compared with control using two-way ANOVA followed by Tukey's test.

Table No.6: Superoxide Dismutase (SOD) Activity of Bark Extracts of Myristica malabarica and Sesbania grandiflora Compared with Standard Ascorbate

Conc. (µg/mL)	EAMM (Bark)	MEMM (Bark)	EASG (Bark)	MESG (Bark)	Standard (Ascorbate)
50	3.2 ± 0.15*	4.5 ± 0.17*	3.5 ± 0.16*	4.9 ± 0.18*	5.3 ± 0.18
100	5.6 ± 0.18**	7.9 ± 0.21**	6.2 ± 0.19**	8.5 ± 0.22**	9.1 ± 0.23
200	8.4 ± 0.22***	11.3 ± 0.25***	9.1 ± 0.23***	12.1 ± 0.26***	13.4 ± 0.28
400	10.7 ± 0.26***	13.8 ± 0.30***	11.4 ± 0.27***	14.7 ± 0.32***	16.2± 0.34

Values are expressed as mean ± SD (n = 3).* p < 0.05, ** p < 0.01, *** p < 0.001 compared with control using two-way ANOVA followed by Tukey's test.

Table No.7: Catalase (CAT) Activity of Bark Extracts of Myristica malabarica and Sesbania grandiflora Compared with Standard Ascorbate

Conc. (µg/mL)	EAMM (Bark)	MEMM (Bark)	EASG (Bark)	MESG (Bark)	Standard (Ascorbate)
50	2.8 ± 0.12*	3.9± 0.13*	3.1 ± 0.13*	4.2 ± 0.14*	4.7 ± 0.1
100	4.9 ± 0.15**	6.7 ± 0.17**	5.2 ± 0.16**	7.1 ± 0.18**	8.0 ± 0.20
200	7.1 ± 0.18***	9.8 ± 0.21***	7.5 ± 0.19***	10.4 ± 0.22***	11.6 ± 0.25
400	9.3 ± 0.22***	12.5 ± 0.26***	10.1 ± 0.24***	13.2 ± 0.27***	14.5 ± 0.29

Values are expressed as mean ± SD (n = 3).* p < 0.05, ** p < 0.01, *** p < 0.001 compared with control using two-way ANOVA followed by Tukey's test.

Table No.8: Reduced Glutathione (GSH) Levels in Bark Extracts of Myristica malabarica and Sesbania grandiflora Compared with Standard GSH

Conc. (µg/mL)	EAMM (Bark)	MEMM (Bark)	EASG (Bark)	MESG (Bark)	Standard (GSH)
50	8.2 ± 0.18*	11.4 ± 0.20*	9.1 ± 0.19*	12.0 ± 0.21*	13.5 ± 0.22
100	12.6 ± 0.22**	16.8 ± 0.25**	13.9 ± 0.23**	18.1 ± 0.26**	20.4 ± 0.27
200	17.3 ± 0.26***	23.5 ± 0.29***	19.2 ± 0.27***	25.7 ± 0.30***	28.8 ± 0.31
400	22.9 ± 0.30***	30.1 ± 0.34***	25.4 ± 0.31***	32.3 ± 0.36***	35.0 ± 0.38

Values are expressed as mean ± SD (n = 3).* p < 0.05, ** p < 0.01, *** p < 0.001 compared with control using two-way ANOVA followed by Tukey's test.

Table No.9: Inhibitory Activity for Lipid Peroxidation forBark Extracts of Myristica malabarica and Sesbania grandiflora by TBARS Assay Compared with Ascorbic Acid

Conc. (µg/mL)	EAMM (Bark)	MEMM (Bark)	EASG (Bark)	MESG (Bark)	Ascorbic Acid (Std)
50	24.2 ± 1.2*	35.5 ± 1.4*	26.1 ± 1.3*	37.3 ± 1.5*	43.2 ± 1.6
100	39.8 ± 1.5**	52.7 ± 1.8**	42.5 ± 1.6**	55.9 ± 1.9**	63.8 ± 2.1
200	56.3 ± 1.9***	74.6 ± 2.1***	58.4 ± 2.0***	77.2 ± 2.2***	83.5 ± 2.4
400	71.6 ± 2.3***	88.3 ± 2.6***	73.9 ± 2.4***	90.5 ± 2.7***	96.0 ± 2.8

Values are expressed as mean ± SD (n = 3).* p < 0.05, ** p < 0.01, *** p < 0.001 compared with control using two-way ANOVA followed by Tukey's test.

Table No.10: Acetylcholinesterase (AChE) Inhibitory Activity of Bark Extracts of Myristica malabarica and Sesbania grandiflora Compared with Donepezil

Conc. (µg/mL)	EAMM (Bark)	MEMM (Bark)	EASG (Bark)	MESG (Bark)	Donepezil (Std)
50	22.6 ± 1.2*	33.4 ± 1.4*	24.3 ± 1.3*	35.2 ± 1.5*	45.1 ± 1.6
100	38.9 ± 1.5**	51.6 ± 1.7**	40.5 ± 1.6**	54.9 ± 1.8**	66.5 ± 2.0
200	55.4 ± 1.8***	73.5 ± 2.0***	57.6 ± 1.9***	76.8 ± 2.1***	87.2 ± 2.3
400	69.7 ± 2.1***	88.1 ± 2.4***	71.8 ± 2.2***	90.4 ± 2.5***	97.8 ± 2.7

Values are expressed as mean ± SD (n = 3).* $p < 0.05$, ** $p < 0.01$, *** $p < 0.001$ compared with control using two-way ANOVA followed by Tukey's test.

Table No.11: List of Phytochemicals identified in methanolic bark extracts of Myristica malabarica and Sesbania grandiflora by HR-LCMS technique

S. No	Molecule	Formula	MW	Rt
1	Ureidoglycine	C3H7N3O3	133.11	1.265
2	3'-O-Methylequol	C16H16O4	272.3	1.318
3	2-Amino-3,4-dihydroxybutanoic acid	C4H9NO4	135.12	1.801
4	n, n'-dinitrosopiperazine	C4H8N4O2	144.13	5.974
5	DMDP	C6H13NO4	163.17	6.07
6	Diethyl (2R,3R)-2-methyl-3-hydroxysuccinate	C9H16O5	204.22	7.04
7	4-Hydroxybenzylamine	C7H9NO	123.15	7.32
8	(R)-Mevalonic acid	C6H12O4	148.16	7.769
9	Pramipexole	C10H17N3S	211.33	7.914
10	Gibberellin Ga115	C20H26O6	362.42	7.955
11	Gabapentin	C9H17NO2	171.24	8.008
12	Androsta-4,9(11)-diene-3,17-dione	C19H24O2	284.39	8.014
13	Methapyrilene	C14H19N3S	261.39	8.23
14	Coronatine	C18H25NO4	319.4	8.317
15	Glycyl-Lysine	C8H17N3O3	203.24	8.345
16	Valclavam	C14H23N3O6	329.35	8.45
17	Cyclopentolate	C17H25NO3	291.39	8.621
18	1,8-Diazacyclotetradecane-2,9-dione	C12H22N2O2	226.32	8.659
19	Glycyl-Histidine	C8H12N4O3	212.21	8.765
20	Dinorcapsaicin	C16H23NO3	277.36	8.868
21	Glutamyl-threonine	C9H16N2O6	248.23	8.946
22	Hypusine	C10H23N3O3	233.31	9.018
23	DL-Ornithino-L-alanine	C8H17N3O4	219.24	9.068
24	Pyronine Y	C17H19ClN2O	302.8	9.275
25	Pivmecillinam	C21H33N3O5S	439.57	9.417
26	Valyl-Methionine	C10H20N2O3S	248.34	9.854
27	Pirenperone	C23H24FN3O2	393.45	10.924
28	Drotaverine	C24H31NO4	397.51	12.196
29	Spiramine A	C24H33NO4	399.52	12.504
30	Linopirdine	C26H21N3O	391.46	12.959
31	4-Hydroxyenterodiol	C18H22O5	318.36	13.604
32	Fludrocortisone	C21H29FO5	380.45	13.73
33	Dihydropteroic acid	C14H14N6O3	314.3	15.613
34	2-Methylcyclododecanone	C13H24O	196.33	17.231

S. No	Molecule	Formula	MW	Rt
35	Valyl-Valine	C10H20N2O3	216.28	17.246
36	Daphnoline	C9H6O4	178.14	22.962

Table No.12: Insilico ADME profile of Phytochemicals

Code	Compound Name	HA	RB	HD	TPSA	C Log P	GI-Ab	BBB	Pgp substrate	log Kp (cm/s)	LV	BS
M1	3'-O-Methylequol	20	2	2	58.92	2.61	High	Yes	Yes	-5.87	0	0.55
M2	4-Hydroxybenzylamine	9	1	2	46.25	0.73	High	Yes	No	-7.06	0	0.55
M3	Gabapentin	12	3	2	63.32	0.79	High	Yes	No	-8.13	0	0.55
M4	Androsta-4,9(11)-diene-3,17-dione	21	0	0	34.14	3.31	High	Yes	Yes	-6.42	0	0.55
M5	Methapyrilene	18	6	0	47.61	2.63	High	Yes	No	-5.86	0	0.55
M6	Cyclopentolate	21	7	1	49.77	2.57	High	Yes	No	-6.13	0	0.55
M7	Dinorcapsaicin	20	8	2	58.56	2.68	High	Yes	No	-6.56	0	0.55
M8	Pirenperone	29	5	0	54.68	3.4	High	Yes	Yes	-6.82	0	0.55
M9	Drotaverine	29	9	1	48.95	4.58	High	Yes	No	-4.93	0	0.55
M10	Spiramine A	29	2	0	48	3.33	High	Yes	Yes	-6.27	0	0.55
M11	Linopirdine	30	5	0	46.09	4.03	High	Yes	Yes	-5.75	0	0.55
M12	2-Methylcyclododecanone	14	0	0	17.07	3.68	High	Yes	No	-4.12	0	0.55

Table No:13 Docking results of compounds against selected biological targets

S. No	Compound	Binding Afiinity (-Kcal/mol) against				
		Acetylcholinesterase (1EVE)	Monoamine Oxidase B (2V5Z)	Cyclooxygenase-2 (5IKQ)	GSK-3β (1Q5K)	Keap1-Nrf2 complex (4IQK)
1	M1	-9.3	-9.3	-7.5	-8.4	-7.7
2	M2	-5.7	-5.5	-5.4	-4.9	-4.8
3	M3	-6.5	-6.6	-5.6	-4.7	-5.4
4	M4	**-12.3**	-8.5	-6.8	-7.6	-8.5
5	M5	-7.7	-7.2	-6.1	-5.7	-5.8
6	M6	-8.9	-8.2	**-7.7**	-6.2	-6.6
7	M7	-8.8	-8.1	**-7.8**	-6.3	-6.5
8	**M8**	**-11.7**	**-11.6**	-6.6	**-8.7**	**-9.4**
9	**M9**	**-11.7**	**-11.6**	-6.7	**-8.7**	**-9.4**
10	M10	-9.2	-6.6	-5.6	-4.8	-6.8
11	M11	-9.8	**-9.6**	-4.6	**-8.5**	**-9.5**
12	M12	-8.3	-7.6	-7.3	-7.2	-6.5
13	Donepezil	-10.7	-	-	-	-
14	Selegiline	-	-7.1	-	-	-
15	Safinamide (IL)	-	-9.8	-	-	-
16	Celecoxib	-	-	-7.9	-	-
17	JMS (IL)	-	-	-8.8	-	-
18	Tideglusib	-	-	-	-9.3	-
19	TMU (IL)	-	-	-	-7.3	-
20	Sulforaphane	-	-	-		-3.9
21	IQK (IL)	-	-	-		-9.9

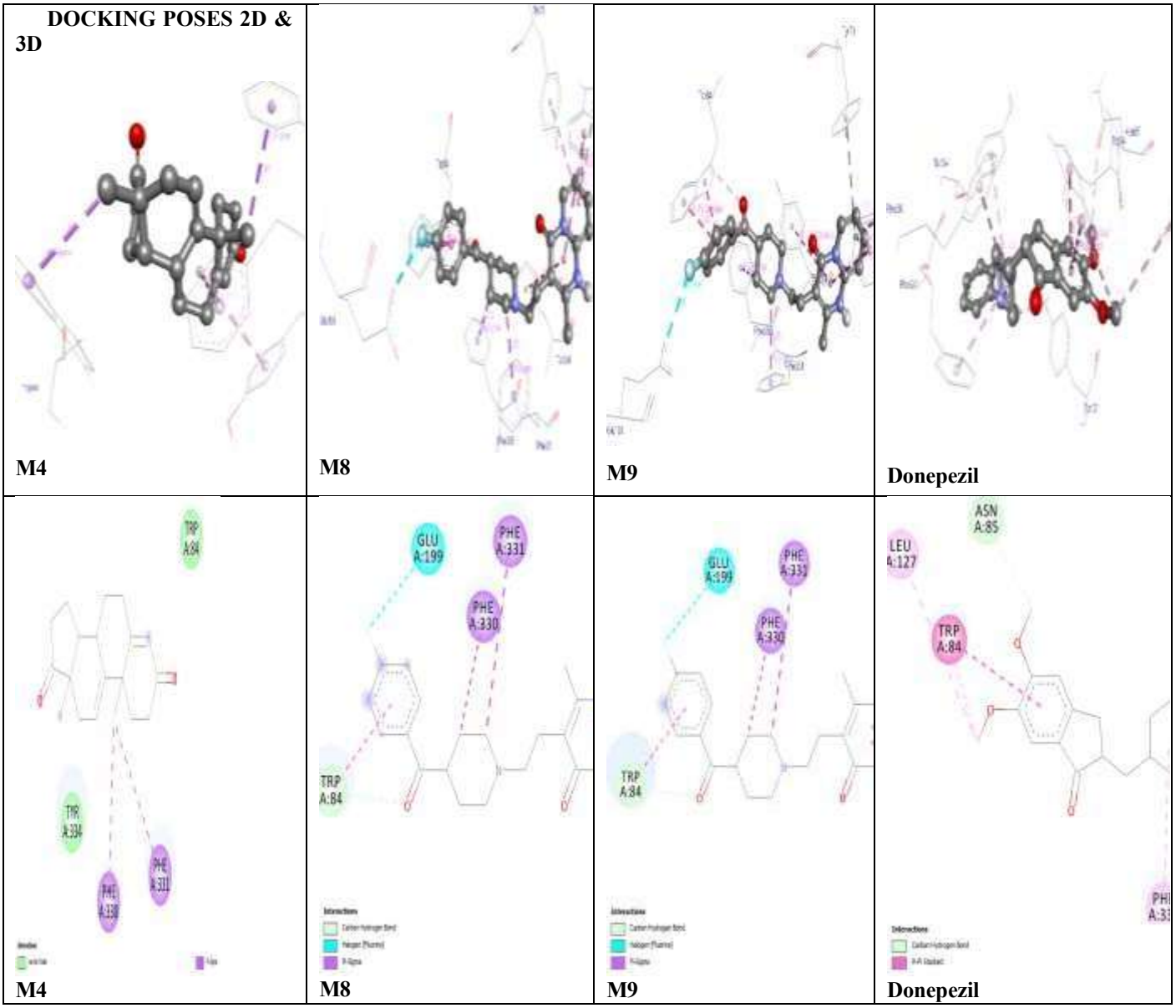

Figure 1: 3D and 2D interactions of selected compounds against Acetylcholinesterase (1EVE)

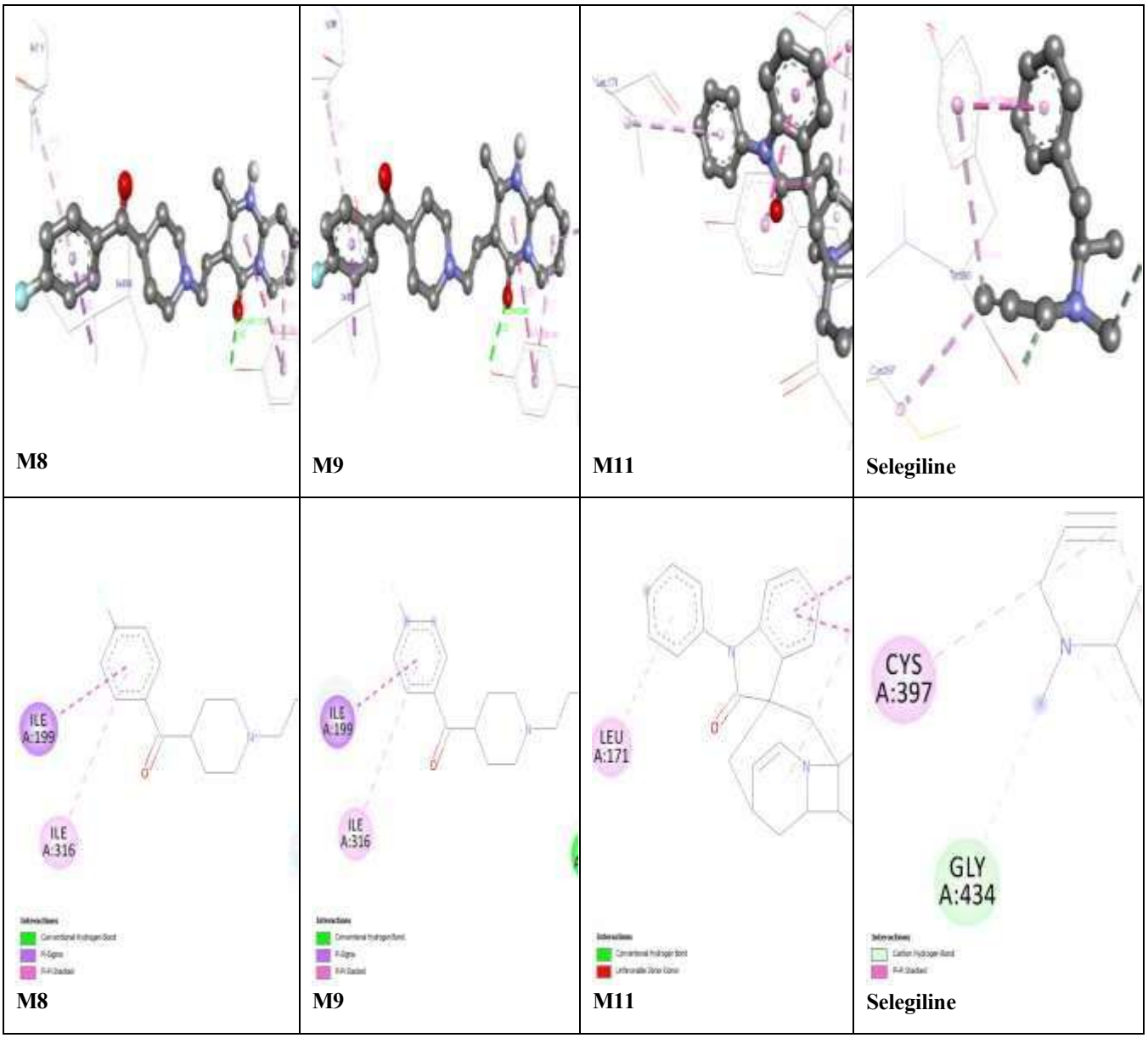

Figure 2 3D and 2D interactions of selected compounds against Monoamine Oxidase B (2V5Z)

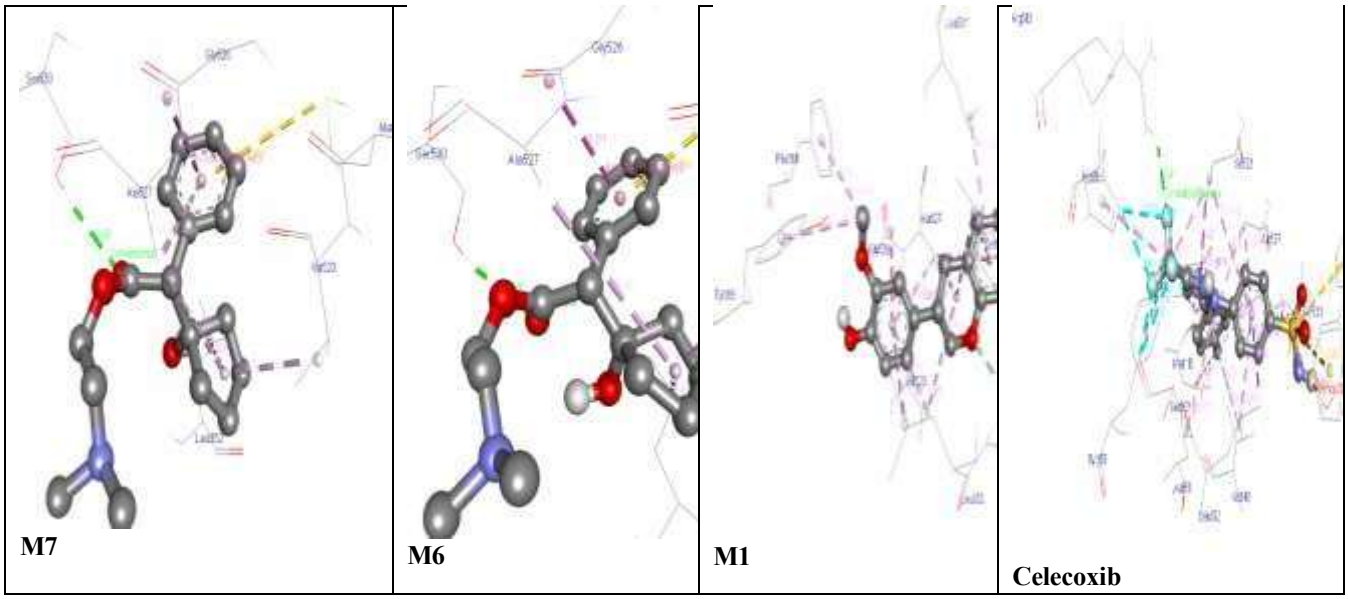

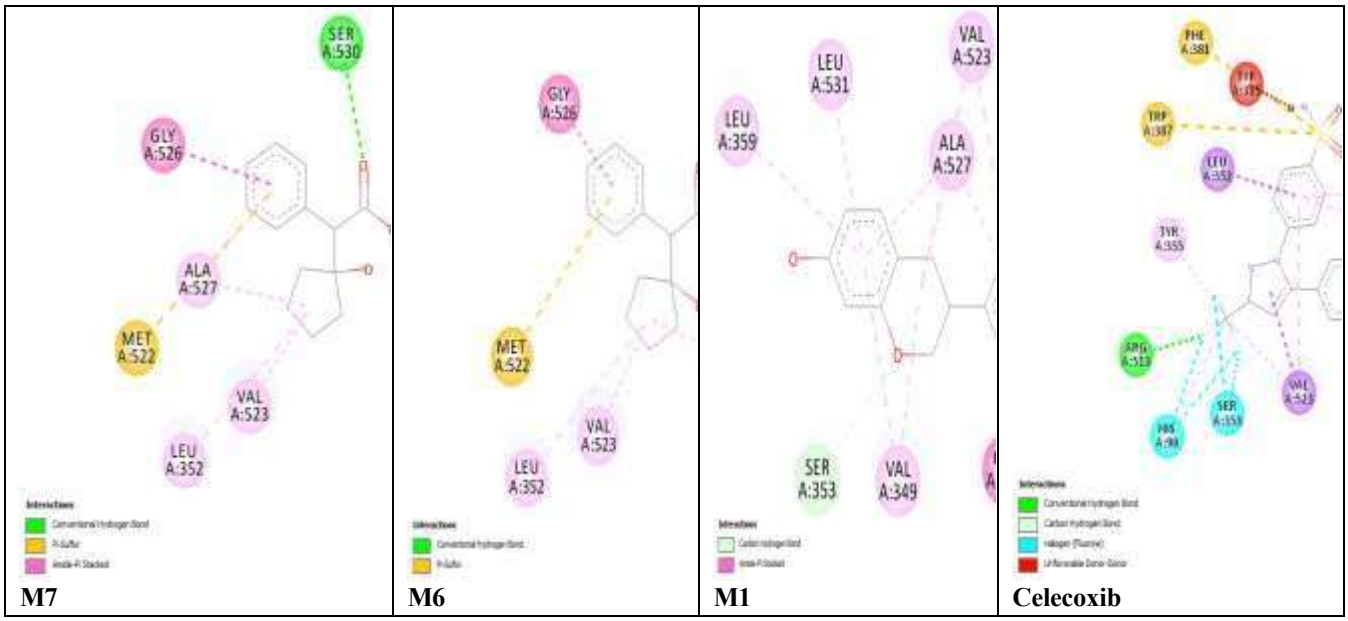

Figure 3: 3D and 2D interactions of selected compounds against Cyclooxygenase-2 (5IKQ)

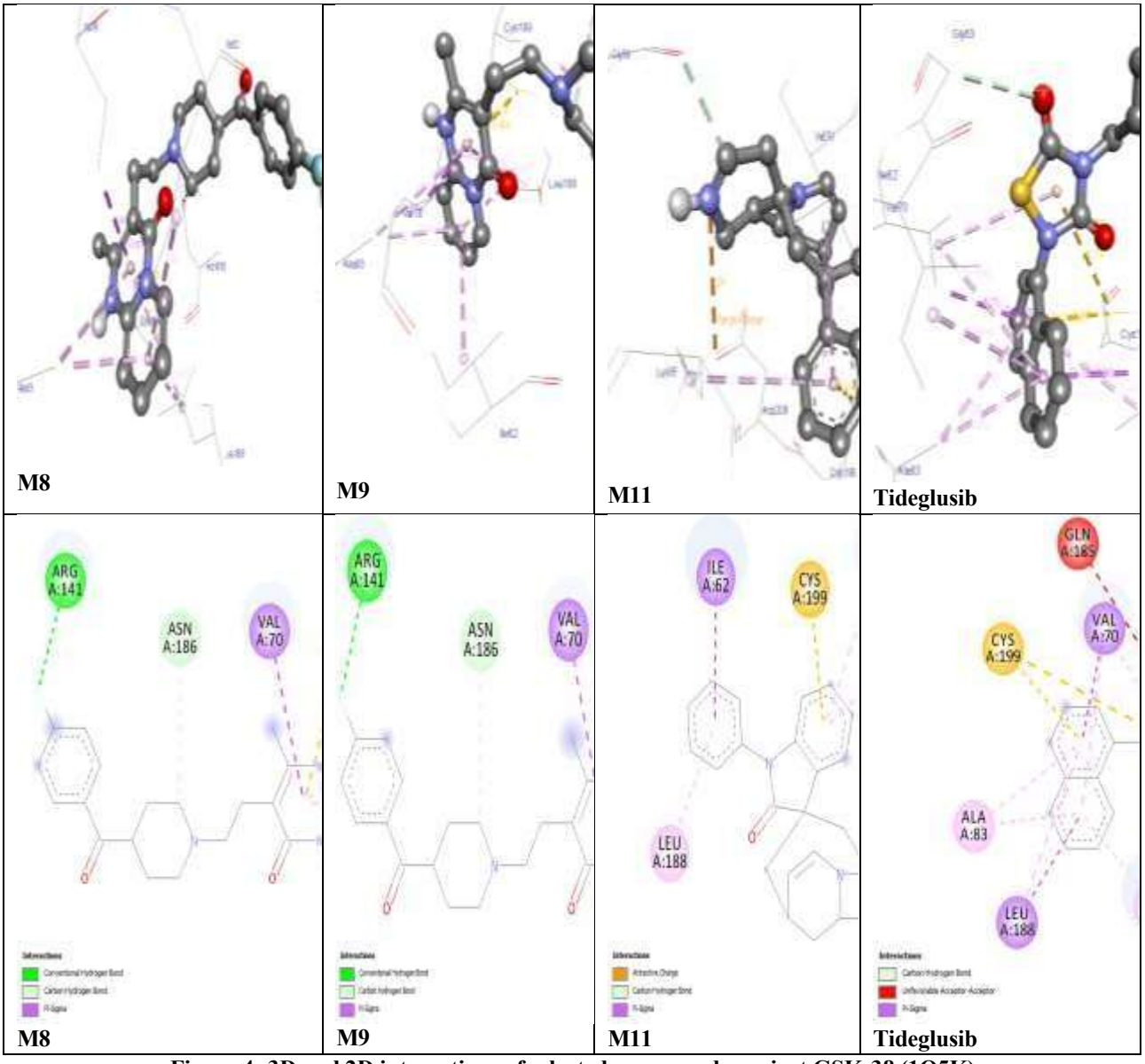

Figure 4: 3D and 2D interactions of selected compounds against GSK-3β (1Q5K)

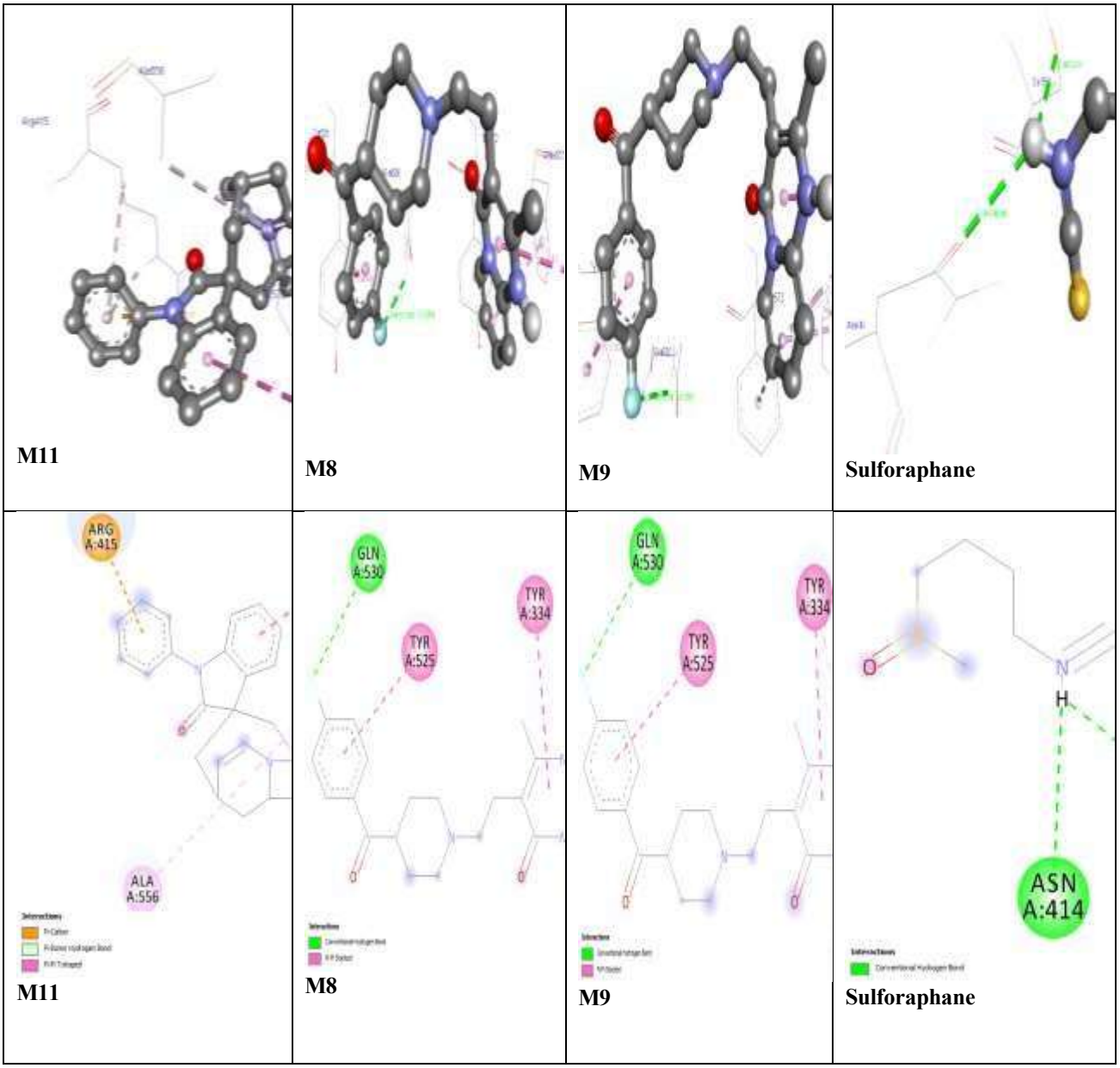

Figure 5: 3D and 2D interactions of selected compounds against Keap1-Nrf2 (4IQK)